Design and Comparative Structure Simulation Analysis of Bandgap Reference Source Based on CMOS 0.18μm Process

Boning Feng [1], Huangshi Su [2,*], Yuzhong Xiang [3]

[1] Arizona College of Technology, Hebei University of Technology, Tianjin, 300000, China

[2] School of Mechanical and Electrical Engineering, Guangdong University of Technology, Guangzhou, Guangdong, 510006, China

[3] School of CHIPS, Xi'an Jiaotong-Liverpool University, Jiangsu Taicang, 215400, China

* Corresponding Author Email: 3122000539@mail2.gdut.edu.cn

Abstract. To address the need for high-precision reference voltages in analog integrated circuits, this paper designs and simulates two bandgap reference structures based on TSMC's 0.18μm CMOS process. First, the operating principle and temperature compensation mechanism of a traditional current mirror-based bandgap reference are implemented and analyzed. Building on this foundation, a bandgap reference containing an operational amplifier is then introduced, and simulations of the two structures are compared. Simulation comparison results on the Cadence Spectre platform show that the op amp-based bandgap reference significantly outperforms the classic current mirror structure in key metrics such as temperature coefficient and power supply rejection ratio (PSRR). The temperature coefficient is reduced from approximately 27.4ppm/℃ to 10.6ppm/℃, the maximum voltage drift is reduced from 5.29mV to 2.24mV, and the low-frequency PSRR is improved from 18.3 dB to 46.5dB. These results demonstrate that the op amp-based structure offers significant advantages in temperature stability and immunity to power supply interference, making it more suitable for use in high-precision analog and mixed-signal circuits.

Keywords: Bandgap reference source, Temperature drift, CMOS process, Voltage reference, Cadence simulation.

1. Introduction

In modern analog and mixed-signal integrated circuits, front-end voltage references, ADCs, LDOs, and other modules are core components of servos. From data converters to power management systems, the stability of the reference voltage directly determines the performance of the entire system. While traditional Zener differential references are simple in structure, their temperature coefficients often exceed 1000ppm/℃, making them difficult to meet the demands of modern integrated circuits.

The bandgap reference (BGR) circuit is designed to provide accurate reference voltage or bias current for other modules and has become one of the core modules in many analog circuits. In 1974, Brokaw first proposed a popular BGR topology [1]. In this topology, a zero-temperature coefficient (zero-TC) voltage circuit is used as a reference voltage generator. In analog devices, the stability of the reference voltage generated by the BGR module plays a vital role in the performance of the entire circuit [2]. For example, the output voltage of a low-dropout linear regulator (LDO) is linearly related to the reference voltage. Therefore, the ripple of the BGR output voltage directly affects the accuracy of the LDO output, which may affect the performance of the integrated circuit using the LDO as a power supply.

With the continuous advancement of CMOS processes, the design of bandgap references faces new challenges. In deep-submicron processes, the reduction in supply voltage limits the dynamic range of traditional structures, and the impact of process variations becomes more significant. At the same time, modern electronic systems place increasing demands on the accuracy of references. Applications such as high-speed ADCs and precision sensors require temperature coefficients to be controlled within 10ppm/℃. These demands have prompted researchers to continuously explore new circuit structures and compensation techniques. As demonstrated in an ultrasound imaging system, the power supply-correlated noise cannot be suppressed evenly after beamforming. Instead, it forms

patterned noise (a "white flashlight" artifact) that depends on the focusing angle, severely degrading image quality. This highlights the value of improving the PSRR of the bandgap reference source through op amp feedback in this paper.

This research is based on the TSMC 0.18μm CMOS process platform. This process node offers an excellent balance between performance, power consumption, and cost, and is widely used in various analog/mixed-signal chips. We first implement and analyze a traditional current mirror bandgap reference. Then, addressing its shortcomings, we propose an improved structure based on an operational amplifier. By combining theoretical analysis and simulation verification, we systematically compare the two structures in terms of temperature stability, power supply rejection, and process adaptability.

2. Bandgap reference source design and principle

The classic bandgap reference source is based on a dual-transistor differential structure. It uses the different current densities of the two transistors to generate ΔV_{BE}, forms a PTAT voltage through a series resistor, and adds it to the V_{BE} (CTAT) of the diode to form the temperature-compensated V_{REF}.

2.1. Brief description of working principle and structural composition

The core principle of the bandgap reference source is to use the positive temperature coefficient (PTAT) and negative temperature coefficient (CTAT) voltages of the bipolar junction transistor (BJT) to compensate each other.

2.1.1 CTAT Voltage

In a bipolar transistor, the relationship between collector current and base voltage is:

$$I_C = I_S \cdot e^{\frac{V_{BE}}{V_T}} \tag{1}$$

The I_S is the saturation current and is strongly related to temperature, and $V_T = \frac{kT}{q}$ is the thermal voltage [3]. From this we can get:

$$V_{BE}(T) \approx V_{G0} - \frac{kT}{q} \ln\left(\frac{I_C}{I_S(T)}\right) \tag{2}$$

Since I_S increases exponentially with temperature, V_{BE} decreases with increasing temperature, which reflects the CTAT characteristic [4].

2.1.2 PTAT Voltage

If the two tubes are operated at different current densities, the voltage difference across the junction is [5]:

$$\Delta V_{BE} = \frac{kT}{q} \ln\left(\frac{J_1}{J_2}\right) \tag{3}$$

From equation (3), we can obtain a voltage ΔV_{BE} that is linearly positively correlated with temperature [6], where J_1, J_2 are the current densities of the two tubes. Since $\frac{kT}{q} \propto T$, it can be seen that ΔV_{BE} is proportional to the absolute temperature, forming a PTAT voltage [4].

2.1.3 Basic principles of bandgap operation

The basic voltage expression of the basic principle of classical bandgap operation is as follows:

$$V_{REF} = V_{BE} + K \cdot \Delta V_{BE} \tag{4}$$

Ideally, by properly selecting the K value, the first-order temperature coefficient can be made zero, and the typical output voltage is about 1.25V (the bandgap voltage of silicon) [7]. The main principle is to control two BJT transistors with an area ratio of n:1 (implemented using MOS equivalent BJT),

resistors R1 and R2 control the PTAT voltage and output amplitude, and finally the current mirror maintains the consistency of the tube current [8].

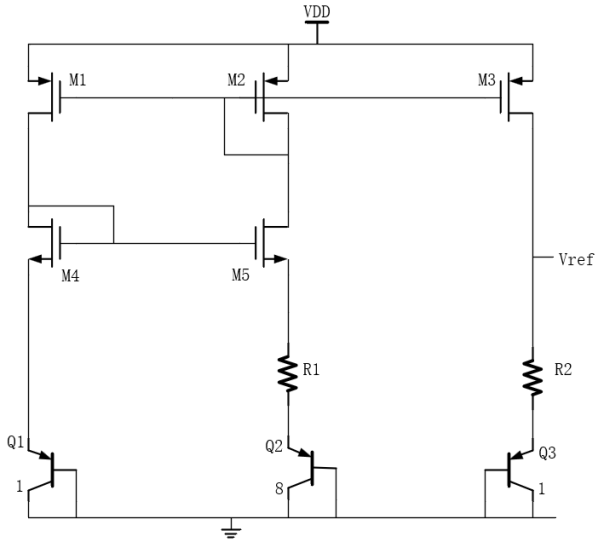

Figure 1. Classic current mirror structure bandgap reference circuit

Figure 1 shows the classic current mirror bandgap reference circuit implemented in this article. The circuit consists of the following key components:

In TSMC 0.18μm process, our design choice is to use bipolar transistor pairs Q1, Q2, and Q3, with an area ratio of 1:8:1. A current mirror network (M1-M5) ensures current matching between the two branches. Resistor networks R1 and R2 provide PTAT voltage generation and output regulation. The supply voltage VDD = 1.8V. In order to make the output voltage V_{REF} conform to the parabola, the resistor R2 = 47K of the current mirror structure is adjusted.

3. Design of Bandgap Reference Source Structure with Op Amp

3.1 Structural characteristics

The main feature of this structure is that the addition of an op amp automatically stabilizes the node voltage, more accurately generates ΔV_{BE}, and makes the output more linear. Secondly, it is extended to second-order temperature compensation and appropriately adjusts the resistor divider to achieve different voltage output targets.

The main innovations of the op amp-based architecture include: A high-gain op amp forces the base voltages of Q1 and Q2 to be equal, precisely controlling the generation of ΔV_{BE}. Second, adaptive bias regulation allows the op amp output to dynamically adjust the gate voltage of the PMOS current mirror, compensating for power supply fluctuations. Finally, space is reserved for second-order compensation resistors to facilitate subsequent curvature correction. This active regulation approach offers improved noise immunity compared to passive current mirrors.

3.2 Structural composition

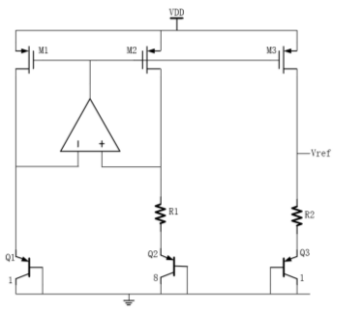

Figure 2. Overall structure diagram with op amp added

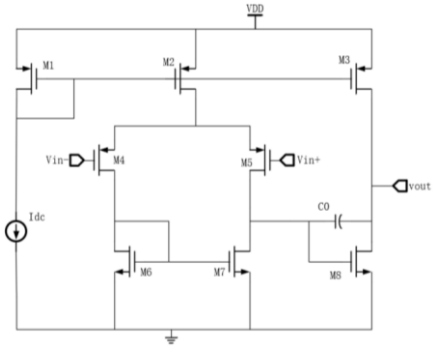

Figure 3. Internal structure diagram with op amp added

The performance simulation diagram of the op amp used in this article is as follows:

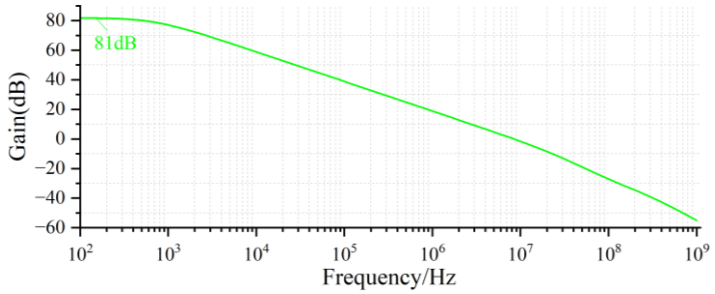

Figure 4. Gain curve

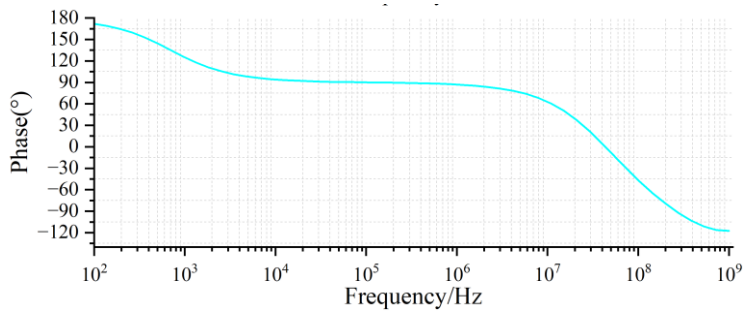

Figure 5. Phase curve

In the structures shown in Figures 2 and 3, an op amp is incorporated into the current mirror to stabilize the base voltage difference, thereby ensuring accurate generation of ΔV_{BE}. Figure 2 shows the overall structure including the op amp, where the op amp maintains current balance by controlling the current mirror, and resistors R1 and R2 set the output voltage V_{REF}. Figure 3 shows the internal circuit of the op amp, which consists of a differential input stage, a current mirror load, and a common-source amplifier output stage. Miller compensation capacitors are added at the output to ensure stability.

Figures 4 and 5 show the gain and phase curves of the op amp, respectively. As can be seen, the op amp's DC gain is approximately 81dB, and its phase margin is approximately 67°, meeting the stability requirements for the core amplifier unit of a bandgap reference circuit. By adjusting resistor R2 (e.g., 53kΩ in this design), the output voltage V_{REF} can be made to better match the theoretical expected value. Overall, the op amp achieves excellent resistance to temperature and power supply fluctuations while maintaining high gain and phase margin.

4. Simulation analysis and result comparison

4.1 Temperature characteristics simulation

This simulation primarily uses Cadence ADE, with a temperature range set to -40°C to 125°C. The simulation extracts the output V_{REF} curve over temperature, ultimately calculating the temperature

drift coefficient (ppm/°C). The temperature drift coefficient of a bandgap circuit is one of the most critical indicators for measuring its core performance.

Temperature coefficient (TC) calculation formula (T belongs to -40 to 125 degrees Celsius):

$$TC = \frac{V_{max} - V_{min}}{V_{mean}(T_{max} - T_{min})} \times 10^6 \quad (5)$$

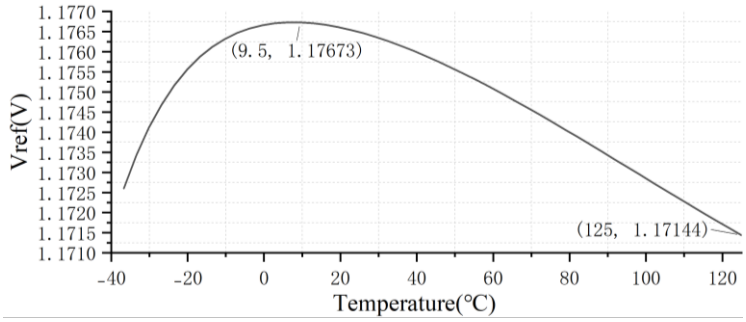

Figure 6. Temperature drift (current mirror structure)

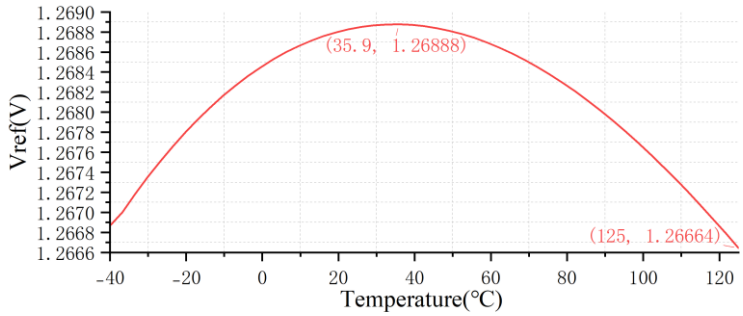

Figure 7. Temperature drift (including op amp structure)

Based on the simulation results of Figures 6 and 7 and using the TC calculation formula, the temperature coefficients of the two structures can be obtained, and Table 1 is plotted accordingly.

Table 1. Comparison of drift and temperature coefficient

Circuit structure	Output voltage (typical)	Maximum drift (mV)	Temperature coefficient (ppm/°C)
Classic structure	1.1726 V	5.29mV	≈ 27.4 ppm/°C
Contains op amp structure	1.2669 V	**2.24**mV	≈ 10.6 ppm/°C
Difference	+8.2%	57.7%	61.3%

Table 1 shows the differences in temperature characteristics between the two structures. Regarding output voltage stability, the maximum drift of the classic current mirror structure is 5.29mV, while the maximum drift of the op amp-based structure is 2.24mV, a difference of 57.7%. Regarding the temperature coefficient, the classic current mirror structure is approximately 27.4ppm/°C, while the op amp-based structure is 10.6ppm/°C, a difference of 61.3%. This shows that the two circuits differ significantly in temperature drift control and temperature coefficient. The op amp-based structure exhibits smaller drift and temperature coefficient, making it more suitable for applications requiring high precision.

4.2 Power Supply Rejection Ratio (PSRR) Analysis

The power supply rejection ratio (PSRR) is an important indicator for measuring the ability of a bandgap reference source to resist power supply noise. It is defined as the sensitivity of the output voltage to changes in the power supply voltage. In the classic current mirror structure, changes in the power supply voltage VDD will directly affect the drain-source voltage of the PMOS current mirror, causing the mirror current to be disturbed due to the finite output resistance r_o. In particular, the

current change of M3 in the right branch will cause the collector current of Q3 to shift, thereby changing VBE3 (the voltage of Q3), and ultimately causing VREF to shift. This is the main reason for the poor low-frequency PSRR of the classic structure. As observed in the ultrasound receiver LNA, the single-ended structure is very sensitive to power supply fluctuations, resulting in poor PSRR performance, which also explains the low PSRR of the classic current mirror bandgap structure in this article [9]. Changes in the current mirror current will directly cause changes in the collector current of the BJT, thereby changing its VBE. Since VREF is composed of VBE3, ΔV_{BE} and the resistor divider, the current change will be amplified to the output end. The improved structure incorporates an operational amplifier, significantly improving PSRR through the following mechanisms:

The op amp forces the voltage across Q1 and Q2 to remain consistent, ensuring that ΔVBE precisely falls across R1. When VDD fluctuations cause mirror current disturbances, the op amp output automatically compensates for the current variation by adjusting the gate voltage of the PMOS current mirror (M1, M2, and M3), leaving ΔV_{BE} largely unaffected. This fundamentally improves low-frequency PSRR.

Within the feedback loop, R1 primarily sets the PTAT current, while R2 determines the weighted ratio of the output voltages. Because the current is stably controlled, R1 and R2 are less sensitive to power supply noise, further improving PSRR.

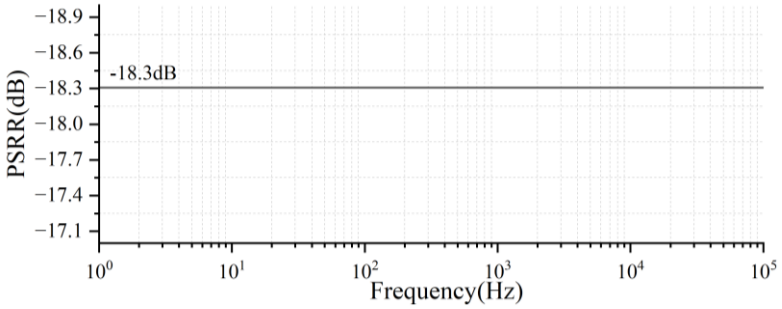

Figure 8. PSRR simulation curve (current mirror structure bandgap)

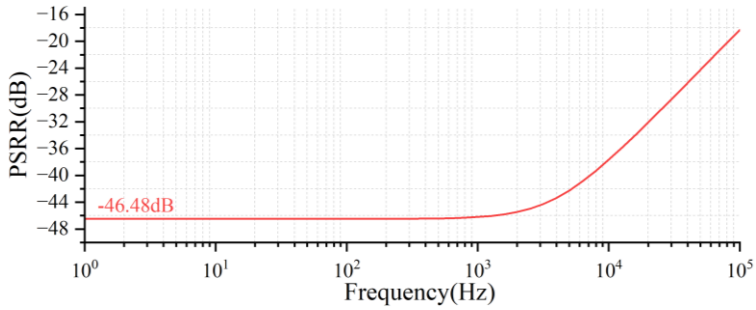

Figure 9. PSRR simulation curve (including op amp band gap)

Figure 8 and Figure 9 show the PSRR curves of the traditional current mirror bandgap structure and the bandgap structure containing an op amp, respectively. The measured results show that the op amp structure proposed in this paper improves the low-frequency PSRR from 18.3dB to 46.5dB. This improvement is mainly attributed to the strong feedback provided by the operational amplifier and the dynamic compensation of the current mirror, which greatly reduces the impact of power supply voltage fluctuations on VREF. The gain exceeds 28dB. This improvement is comparable to the PSRR improvement achieved by LDOs using feedforward technology (e.g., 26.5dB at 1MHz) [10], which together verify the effectiveness of active compensation technology in suppressing power supply noise. As the frequency increases, the loop gain decreases, and the difference in PSRR between the two structures gradually decreases, but the improved structure still performs significantly better than the classic current mirror version below 100kHz.

4.3 Circuit Performance Comparison and Summary

Comparing the simulation results for 4.1 Temperature Characteristics and 4.2 Power Supply Rejection Ratio (PSRR) reveals significant differences between the two structures across various performance dimensions, yet common patterns also exist. First, both the classic current mirror structure and the improved structure with op amps achieve basic bandgap reference functionality, and under the same process platform and simulation conditions, the output voltage exhibits consistent trends with temperature and power supply variations. Second, the introduction of the op amp significantly improves both core performance indicators: in terms of temperature characteristics, the maximum drift is reduced from 5.29mV to 2.24mV, and the temperature coefficient is optimized from 27.4ppm/°C to 10.6ppm/°C, representing improvements of 57.7% and 61.3%, respectively. In terms of power supply rejection ratio, the low-frequency PSRR increases from 18.3dB to 46.5dB, with a gain exceeding 28dB. This demonstrates that op amp feedback not only enhances the ΔV_{BE} matching accuracy but also effectively suppresses the impact of power supply voltage disturbances on the output.

5. Conclusion

This article compares two bandgap reference structures implemented in TSMC's 0.18μm CMOS process: a traditional current mirror structure and an op amp-based structure. Temperature characteristics and power supply rejection ratio (PSR) simulations were performed under identical conditions. The traditional current mirror structure exhibits a temperature coefficient of approximately 27.4ppm/°C and a maximum voltage drift of 5.29mV over the -40°C to 125°C range. The op amp-based structure demonstrates better temperature compensation, with a temperature coefficient of 10.6ppm/°C and a maximum drift of 2.24mV. The traditional current mirror structure achieves a PSRR of approximately 18.3dB at low frequencies, while the op amp-based structure achieves 46.5dB, significantly enhancing its ability to suppress power supply fluctuations. While both structures can achieve basic bandgap reference functionality, the op amp-based structure demonstrates superior performance in temperature drift control and power supply interference rejection. The bandgap reference source with op amp exhibits better stability and reliability while maintaining low power consumption and process compatibility, providing strong support for its application in high-precision analog circuit design.

Authors Contribution

All the authors contributed equally and their names were listed in alphabetical order.

References

[1] Ma B, Yu F. A novel 1.2–V 4.5-ppm/◦C curvature-compensated CMOS bandgap reference [J]. IEEE Transactions on Circuits and Systems I: Regular Papers, 2014, 61 (4): 1026-1035.

[2] Fu X, Colombo D M, Yin Y, El-Sankary K. Low noise, high PSRR high-order piecewise curvature compensated CMOS bandgap reference [J]. IEEE Access, 2022, 10: 110970-110982.

[3] Razavi B. Simulation-based CMOS integrated circuit design [M]. Chen Guican, et al., trans. Xi'an: Xi'an Jiaotong University Press, 2003.

[4] Wei Rongshan, Zhong Meiqing. Design of bandgap reference circuit with low power supply voltage [J]. Electronic Science and Technology, 2017 (1): 34-36.

[5] Brokaw A P. A simple three-terminal IC bandgap reference [J]. IEEE Journal of Solid-State Circuits, 1974, 9 (6): 388-393. DOI: 10.1109/JSSC.1974.1050532.

[6] FAKHARYAN I, EHSANIAN M. A sub-1V nanowatt CMOS bandgap voltage reference with temperature coefficient of 13 ppm/°C [J]. 23rd Iranian Conference on Electrical Engineering, 2015.

[7] Wang Siyuan, Zhang Guoheng, Ma Wenhao, et al. Design of a low-power bandgap reference voltage source [J]. Journal of Northwest Minzu University (Natural Science Edition), 2025, 46 (2): 7-14. DOI: 10.14084/j.cnki.cn62-1188/n.2025.02.009.

[8] Tang Wei, Ma Shanshan, Mu Xinhua, et al. A high PSRR bandgap reference source with quick startup capability [J]. Journal of Xi'an University of Posts and Telecommunications, 2021, 26 (1): 54-59. DOI: 10.13682/j.issn.2095-6533.2021.01.009.

[9] P.Wang, C. Ma, C. Chen, Z. Hong, and J. Xu, “A 65.9-dB PSRR, compact LNA array for correlated noise compression in high-channel-count pitch-matched ultrasound ASICs,” IEEE J. Solid-State Circuits, vol. 60, no. 7, pp. 2294–2304, Jul. 2025.

[10] Y.Lu, T.-A. Yen, R. D. Nayak, S. Alevoor, B. Talele, S. Patil, K. Kunz, and B. Bakkaloglu, “A novel parallel feed-forward current ripple rejection (PFFCRR) technique for high load current high PSRR nMOS LDOs,” IEEE Trans. Very Large Scale Integr. (VLSI) Syst., vol. 33, no. 3, pp. 651–661, Mar. 2025.